Journal of Forestry Research (2014) 25(2): 385−392
DOI 10.1007/s11676-014-0466-x

ORIGINAL PAPER

Satellite monitoring of land-use and land-cover changes in northern Togo protected areas

Fousseni Folega • Chun-yu Zhang • Xiu-hai Zhao • Kperkouma Wala
Komlan Batawila • Hua-guo Huang, Marra Dourma • Koffi Akpagana

Received: 2012-03-22; Accepted: 2013-01-23

Abstract: Remote-sensing data for protected areas in northern Togo, obtained in three different years (2007, 2000, and 1987), were used to assess and map changes in land cover and land use for this drought prone zone. The normalized difference vegetation index (NDVI) was applied to the images to map changes in vegetation. An unsupervised classification, followed by classes recoding, filtering, identifications, area computing and post-classification process were applied to the composite of the three years of NDVI images. Maximum likelihood classification was applied to the 2007 image (ETM+2007) using a supervised classification process. Seven vegetation classes were defined from training data sets. The seven classes included the following biomes: riparian forest, dry forest, flooded vegetation, wooded savanna, fallows, parkland, and water. For these classes, the overall accuracy and the overall kappa statistic for the classified map were 72.5% and 0.67, respectively. Data analyses indicated a great change in land resources; especially between 1987 and 2000 probably due to the impact of democratization process social, economic, and political disorder from 1990. Wide-scale loss of vegetation occurred during this period. However, areas of vegetation clearing and regrowth were more visible between 2000 and 2007. The main source of confusion in the contingency matrix was due to heterogeneity within certain classes. It could also be due to spectral homogeneity among the classes. This research provides a baseline for future ecological landscape research and for the next management program in the area.

Key words: land change, NDVI, land cover, protected areas, Northern Togo

Project funding: This work was supported by the Chinese Ministry of Sciences and Technology -- the host of China-Africa Science and Technology Partnership Program (CASTEP) and the National Special Research Program for Forestry Welfare of China (201104009).

The online version is available at http://www.springerlink.com

Fousseni Folega ( )[1,2*], Chun-yu Zhang[1], Xiu-hai Zhao[1], Kperkouma Wala[2], Komlan Batawila[2], Hua-guo Huang[1], Marra Dourma[2], Koffi Akpagana[2]
[1] The Key Laboratory for Silviculture and Conservation of Ministry of Education, Beijing Forestry University, Beijing100083, People's Republic of China; [2] Université de Lomé, Laboratoire de botanique et écologie végétale, Faculté des sciences, BP 1515, Lomé, Togo.
E-mail: ffolegamez@live.fr; Tel: 008613488679682/0022890106797

Corresponding editor: Chai Ruihai

Introduction

The current reduction and degradation of vegetation cover in sub-Saharan Africa, particularly in its Sudanian zone, have become a major concern for scientists, decisionmakers and local stakeholders. The reduction of vegetation cover appears to be related to both climate variability (Oba et al. 2001) as well as social and economic changes for rural areas across the African continent in recent decades.

Wooded vegetation zones around settlements in Africa, especially in the western part, used to be protected by traditional management systems, organized around local divinities (gods) that were associated with the woodland (Kokou and Sokpon, 2006). Formal boundaries, around such wooded areas in Togo, were put in place during colonization and afterward (Folega et al. 2010; Tchamie 1994).

In Togo, three important periods with respect to the dynamics and demarcation of protected areas can be highlighted. The first one, which extended up from colonial and postcolonial period to 1990, was characterized by conservation and protection of plant and animal resources. However, the management system used at this time was semi-military and very repressive for local human populations. The second period, which extended from 1990 to 2000, was marked by illegal and anarchic exploitation of protected resources by human populations bordering the protected areas. This situation resulted from the political, economic and social troubles of 1990 mainly due to uncontrolled democratic opening process. Illegal activities during this period included forestry harvest; poaching; transhumance (a seasonal change in grazing lands); slash and burn; and farming. The last period, which began after 2000, was characterized by the limitation of illegal practices associated with consensual rehabilitation of

protected areas (UICN / PACO, 2008). The project re-established the boundaries of the existing protected areas that had been the least disturbed during the previous decade (1990–2000). The most disturbed areas were handed over to the populations bordering the areas (Folega et al. 2011a).

Land-use and land-cover data is a valuable source of information for assessment of the natural resources in a country and as a basis for environmental planning (Igue et al. 2006). It also provides a better understanding of landscape dynamics and thus allows better management of their resources.

Up-to-date analyses of land-cover dynamics for these redefined, protected areas in Togo will provide important data resource for solving the current complex environmental issues. . Remote-sensing data (e.g., Landsat imagery, Spot imagery) are suitable for mapping the status of land-cover features (Andrieu and Mering 2008; Baldyga et al. 2007). Land-cover and land-change maps at moderate scales enable researchers to characterize spatial-distribution patterns of land cover. The patterns of land-cover change that have occurred over time can also be quantified. These maps can serve as baseline data for future land cover, ecology, landscape, and area management studies.

This research aims to provide preliminary information on land use and land cover essential for vegetation monitoring and management. The objectives were to assess changes in land cover using a vegetation index and to generate a map of current land cover types from recent remote-sensing data. Knowledge of land-cover features of these protected areas in Togo in the context of their re-qualification and re-demarcation are essential for their sustainable management.

Material and methods

Study Areas

The survey area covers the protected areas of Barkoissi (2000 ha), Galangashi (7500ha) and Oti-Keran (163640ha). These were classified as protected areas on 1 January 1954, 14 September 1954 and 28 September 1950, respectively. The study area encompasses the limit of the first demarcation of these protected areas (Sournia et al. 1998). They are situated in eco-floristic zone 1 (Ern 1979), which is dominated by savanna on leached; ferruginous tropical soils (Fig. 1).

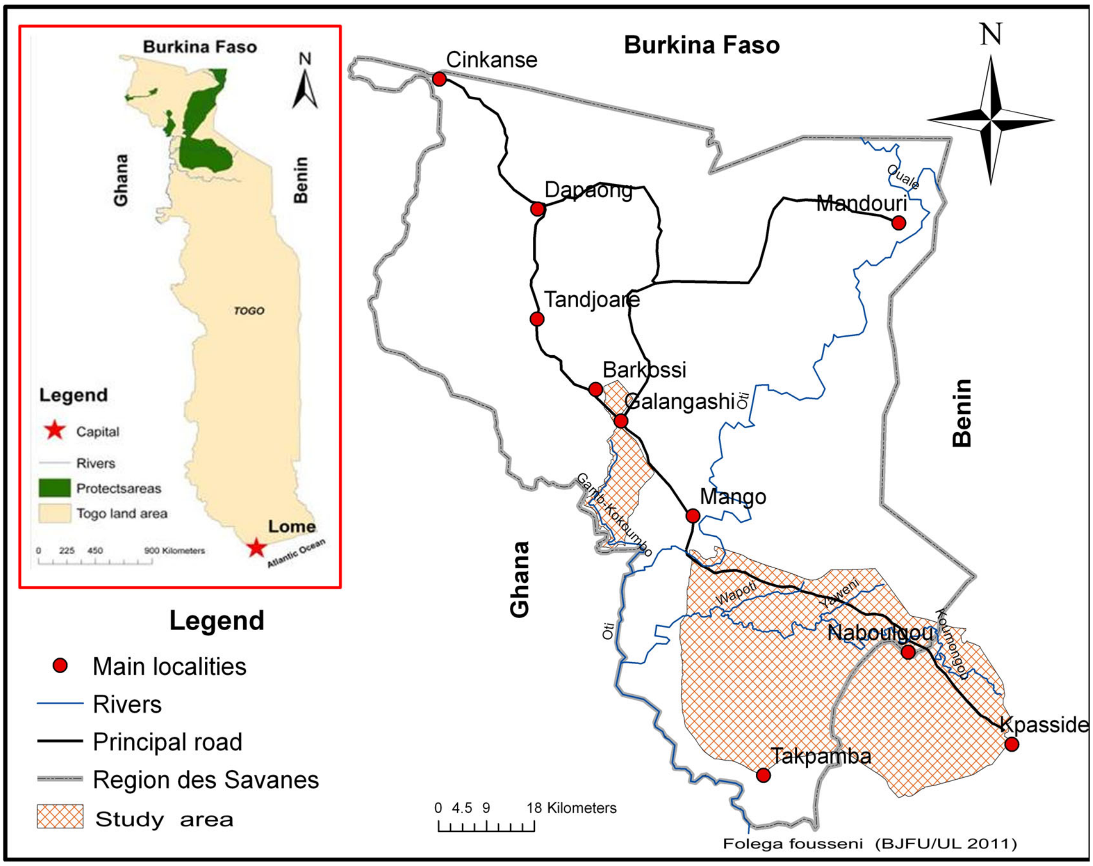

Fig. 1: Study area (PA of Barkoissi, Galangashi and Oti-Keran)

The study area is located between latitude 11°N and 10°N and longitude 0°E and 1°E. The main geomorphological structure relief within the study area is formed by a vast plain, which is dominated by leached, ferruginous soils covering hardpan. The area is drained by two famous rivers, the Oti and the Koumongou. The region has a Sudanese tropical climate marked by the long dry season and short rainy season (Yema et al., 1981). Heavy rains occur in August (Moussa, 2008). The rainfall averages

around 1060 mm per year. Temperatures vary between 20 °C and 35°C, with an annual average of 28.5 °C at the Mango meteorological station (Moussa, 2008).

The major human activities are agriculture, firewood collection, and agricultural fires during the dry season. The main crops are sorghum, millet, groundnuts, cowpeas, maize, and yams. Livestock in the area include cattle, goats and sheep.

The ethnic groups living in the study area include: the Ngamgam, Tchokossi, Lamba, Fulani, Tamberma, Gnande, Moba, and Mossi.

Remote-sensing data, ancillary data, and ground-truth

The remote-sensing data used were Landsat images downloaded from the website of the Global Land Cover Facility (http://www.glcf.umd.edu/data/;http://glcfapp.glcf.umd.edu:8080/esdi/index.jsp). The remote-sensing data covered three periods and consisted of:

- Thematic Mapper (TM) p193/r052 dated 30/10/1987
- Enhanced Thematic Mapper plus (ETM+) p193/r053 dated 04/12/2000
- Enhanced Thematic Mapper plus (ETM+) p193/r053 dated 06/11/2007

Most Landsat 7 images present some problems since the sensor started malfunctioning in May 2003, resulting in images that are striped. For the Landsat 7 scene (p193/r053 dated 06/11/2007) used in this study, stripes were located at the edge of the image but did not affect the study areas, for which data were extracted with a mask using ArcGIS 9.2.

Ancillary data used to recognize the patterns and features of the remote-sensing data were composed mainly of ground reference data obtained from land surveys carried out with a handheld GPS (Garmin, GPSMAP® 60CS), Google Earth online resources, a general map of Togo, and a vegetation map of Togo (Afidegnon et al., 2003).

Ground-truthing from field informations provided training data for the classified image and testing for accuracy assessment of the classification output. The field work took place over two periods, first in the rainy season (August 2009) and second in the dry season (March 2011). It also provided *in situ* information on the dynamics in the area and the main disturbances (grazing, farming, agriculture fire, clearing) leading to land-cover changes. Homogeneous areas on satellite images and in the field were selected. In totally, 160 sample sites in the field were selected with their coordinates. These coordinates were used to assess the accuracy of vegetation type classification. These GPS (Garmin, GPSMAP® 60CS) records were set according to the Universal Transverse Mercator with a WGS84 datum coordinate system.

Land-cover type definitions

Land-cover definitions were based on the previous vegetation classes defined by Afidegnon et al. (2003). The following land-cover types were used: riparian forest (RF); flooded vegetation (FV); wooded savanna and dry forest (WS/DF); mosaic savanna (MS); fallows and parkland (FP); cropland and parkland (CP); and water (W).

Data analysis and interpretation

RGB-NDVI analysis of three Landsat images

The RGB-NDVI method (Sader and Winne, 1992) was used for change detection, as this approach has been found to be more accurate and efficient for analyses of Landsat multi-temporal TM imagery compared to principal component analysis and image differencing (Hayes and Sader, 2002; Wilson and Sader, 2002). Several steps were necessary for this method.

After data acquisition, the bands of each scene were stacked. The three Landsat raw scenes were subjected to geometric calibration verification to geo-reference the images. A haze-reduction algorithm, from Erdas imagine 9.2, was applied to the three scenes (TM_1987, ETM+_2000 and ETM+_2007) to reduce the effect of atmospheric scattering on the data. Haze-correction algorithms are recommended when calculating band ratios or when comparing data from different dates (Chavez and MacKinnon, 1994; Chavez, 1996; Kwarteng and Al-Ajmi, 1996).

The normalized difference vegetation index (NDVI) (Rouse et al. 1974; Tucker, 1979) was then calculated for each image using the following equation:

$$NDVI = \frac{NIR - R}{NIR + R} \tag{1}$$

where, *NIR*: near-infrared; *R*: red.

Generally, NDVI separates green vegetation from other surfaces feature because the chlorophyll of green vegetation absorbs red light for photosynthesis while it reflects the near-infrared wavelengths owing to scattering caused by internal leaf structure (Tucker, 1979). NDVI values are represented as a ratio ranging in value from -1 to 1. Extreme negative values represent water; while values close to zero refer to barren areas of rock, sand, or snow. Low and high positive values indicate leaf biomass, such as grassland, shrubland, or temperate and tropical rainforest (Sellers, 1985; Wilson and Sader, 2002).

The three NDVI images obtained (NDVI_87, NDVI_00 and NDVI_07) were stacked to get a new image of the three layers. This new image was formed from a red, a green, and a blue layer, which corresponded to the NDVI_87, NDVI_00 and NDVI_07 images, respectively.

Among the several different unsupervised classification algorithms commonly used in remote sensing, the ISODATA (*Iterative Self-Organizing Data Analysis Technique*) clustering algorithm was chosen for this study because of its additional refinements in terms of splitting and merging clusters (Jensen, 2005). The NDVI image obtained by stacking the layers for different years (RGB_NDVI_870107) was subjected to unsupervised classification using the ISODATA algorithm (Lillesand et al., 2008; Tou and Gonzalez, 1974).

Finally, the 50 thematic classes generated by the unsupervised classification were post-classified. The 50 classes were clustered in nine new classes through class recoding. The recoding was

followed by a spatial filter that aims to consolidate patch boundaries and reduce the visual effects of small patches before computing the areas of each class (Ola, 2008).

Supervised classification of 2007 ETM+ using maximum likelihood classification

A systematic method was used for supervised classification. First, unsupervised classification was applied (ISO-DATA Algorithm) to the ETM+ 2007 image. The classification provided a synoptic view of the spectral signatures, which helped to define the types and extent of ground cover prior to field work (Folega et al., 2011a).

One hundred ground check points were then chosen from the image according to the 10 land-cover classes defined by the previous classification. After field surveys of the ground check points during the rainy season (August 2009) and dry season (March 2011), seven vegetation classes (RF, FV, WS/DF, MS, FW, CP, and W, see above) were defined and used as training sites.

Subsequently, supervised classification was applied to the image based upon the training sites representing the seven vegetation classes. To increase the accuracy of the classification, maximum likelihood classification was applied to the ETM+2007 image. Maximum likelihood classification considers both the variances and covariances of the class signatures when assigning each cell to one of the classes represented in the signature file. The algorithm used by the maximum likelihood classification combines cell assignments to classes in multidimensional space and Bayes' theorem (1763) of decisionmaking.

Accuracy assessment was performed on the 2007 land cover maps. The number of reference pixels in this process is an important factor in determining accuracy. In total, 160 reference pixels were selected for the land-cover maps. The overall accuracy and Kappa analysis were used to determine classification accuracy based on error matrix analysis (Congalton and Green, 1999). The overall accuracy was calculated by summing the number of pixels classified correctly and dividing them by the total number of pixels. Kappa analysis is a discrete multivariate technique used in accuracy assessment (Foody, 2002; Sun et al., 2009). The Kappa coefficient of agreement (K_{hat}) is a measure of accuracy between the classified image and the reference data (Congalton, 1991). It is computed using the following equation:

$$K_{hat}=\frac{N^2\sum_{i=1}^{k}x_{ii}-\sum_{i=1}^{k}(x_{i+}\times x_{+i})}{N^2-\sum_{i=1}^{k}(x_{i+}\times x_{+i})} \tag{2}$$

where k is the number of rows in the matrix, x_{ii} is the number of observations in row i and column i, x_{i+} and x_{+i} are the marginal totals for row i and column i, respectively, and N is the total number of pixels.

K_{hat} values ≥0.81 represent almost perfect accuracy between the classification map and the reference information. K_{hat} values between 0.80 and 0.61 represent substantial agreement. K_{hat} values between 0.60 and 0.41 represent moderate agreement. Values between 0.40 and 0.21 represent fair agreement. K_{hat} values between 0.20 and 0.01 represent slight agreement, while values ≤ 0.01 represent less than chance agreement (Anthony et al., 2005).

Results

Land cover and land use change dynamics

The results for land cover and land use dynamics of the three protected areas are clearly shown in Table 1 and Fig. 2. The different colors displayed in Fig. 2 visually represent the level of change in NDVI values, while Table 1 shows the changes in NDVI values, in terms of the nine colors from which the RGB_NDVI image is composed, and in vegetation cover over 20 years.

Current Land Use and Land Change

Analysis and image classification accuracy are shown in Table 2, which shows the level of precision for each class and the main areas of confusion. The overall accuracy (72.51%) and Kappa statistic index (0.67) computed from the contingency matrix were significant. The Kappa statistic was calculated using the results of the land cover classification with the seven land cover classes shown in the confusion table (Table 2). The distribution of the seven class of land cover is shown through the Fig. 3.

Table 1: Analysis of the vegetation change based on additive color after post-classification

Class color	NDVI Values			Class dynamic over the time	Class area (ha)	Class area (%)
	R	G	B			
Red	H	L	L	Biomass lost (87-00)	30220.1403	15.0253597
Cyan	L	H	H	Biomass: lost before 87 and regeneration between 87-07	25237.1976	12.5478561
Yellow	H	H	L	Biomass: lost between 00-07	11659.5526	5.79709326
Blue	L	L	H	Biomass:lost before 87 and regeneration between 00-07	33514.7968	16.663452
Magenta	H	L	H	Biomass: lost between 87-00 ,regrowth between 00-07	40924.8703	20.3477182
Green	L	H	L	Biomass: lost before 87 ,regrowth between 87-00 and lost between 00-07	29992.73	14.912292
Black	L	L	L	No change: Barren areas, urban area or water	8604.57126	4.27816606
Dark gray	L	L	L	No change: Stable vegetation (Low biomass)	11947.2522	5.94013663
White	H	H	H	No change: Stable vegetation (High biomass)	9026.45494	4.48792531
Total					201127.566	100

H: high value of NDVI; L: low value of NDVI

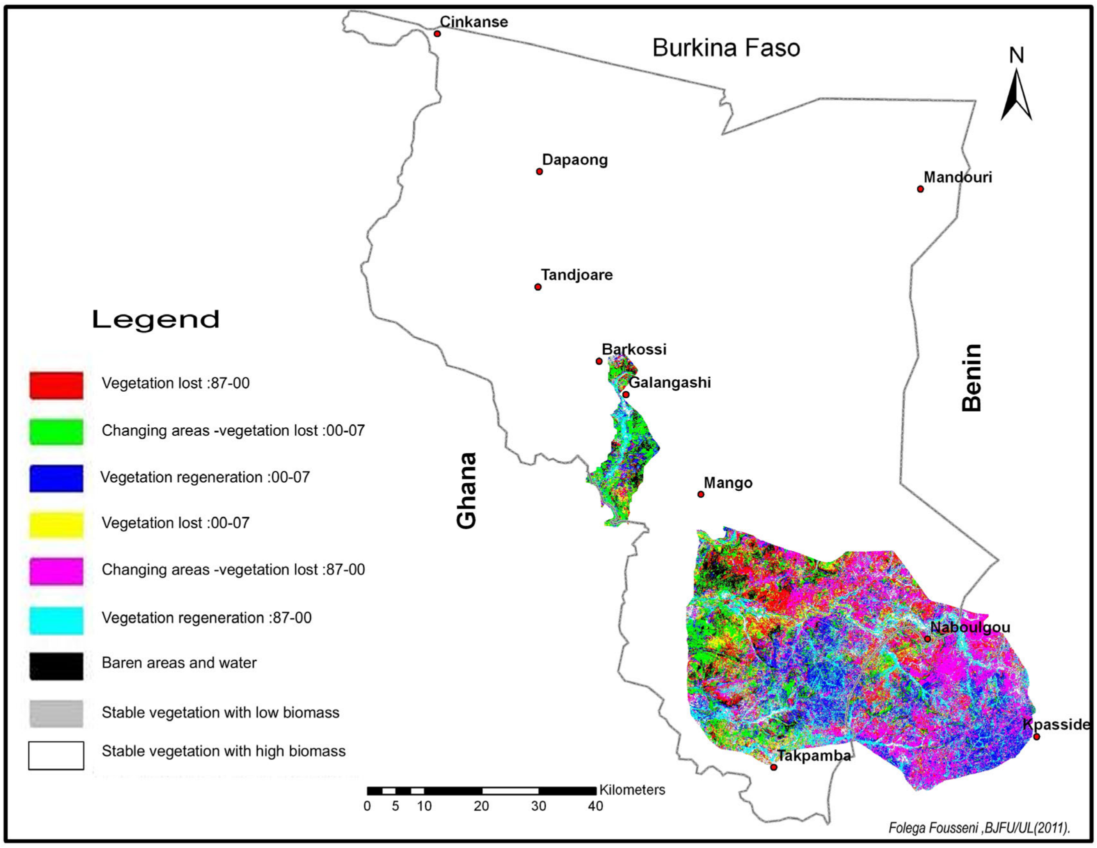

Fig. 2: RGB-NDVI classified map showing the dynamics of Land Cover change in Barkoissi, Galangashi and Oti-Keran PA

Table 2: Confusion Matrix and Kappa Index

	Cropland and Parkland	Fallows and Parkland	Mosaic Savanna	Wooded Savanna and Dry Forest	Riparian Forest	Flooded Vegetation	Water	Total	Producer's Accuracy (%)	User's Accuracy (%)
Cropland and Parkland	**14**	4			1	1		20	73.68	70
Fallows and Parkland		**13**	4					17	76.47	76.47
Mosaic Savanna	2		**18**	2	2	1		25	78.26	72
Wooded Savanna and Dry Forest			1	**11**	7			19	61.11	57.89
Riparian Forest	3			5	**34**			42	68	80.95
Flooded Vegetation					1	**14**		15	66.66	93.33
Water					5	5	**12**	22	100	54.45
Total	19	17	23	18	50	21	12		160	
Overall Accuracy									**72.51%**	
Overall Kappa statistics									**0.67**	

Rows represent grounds data while columns represent image data.

The main areas of confusion encountered during this classification process for the ETM+2007 image related to the spatial configuration of mixed croplands, parklands, fallows, and the different stages of secondary succession of savanna.

Discussion

Change in land use of the three protected areas

Fig. 2 clearly shows and quantifies major decreases or increases in green biomass associated with forest harvest or regrowth. Red and yellow areas represent a decrease in NDVI values (see also Table 1). These colors indicate vegetation loss, usually due to the harvest of plant resources. Vegetation loss between 1987 and 2000 was estimated to be 30220.1403 ha, while between 2000 and 2007 it was 11659.5526 ha (Table 1). Vegetation loss between 1987 and 2000 was probably the result of social, economic, and political disorder from 1990. From observations made in the field, this vegetation loss has continued after 2000 until the present day, and this may be due to the lack of or insufficient moni-

toring and protection measure in these areas.

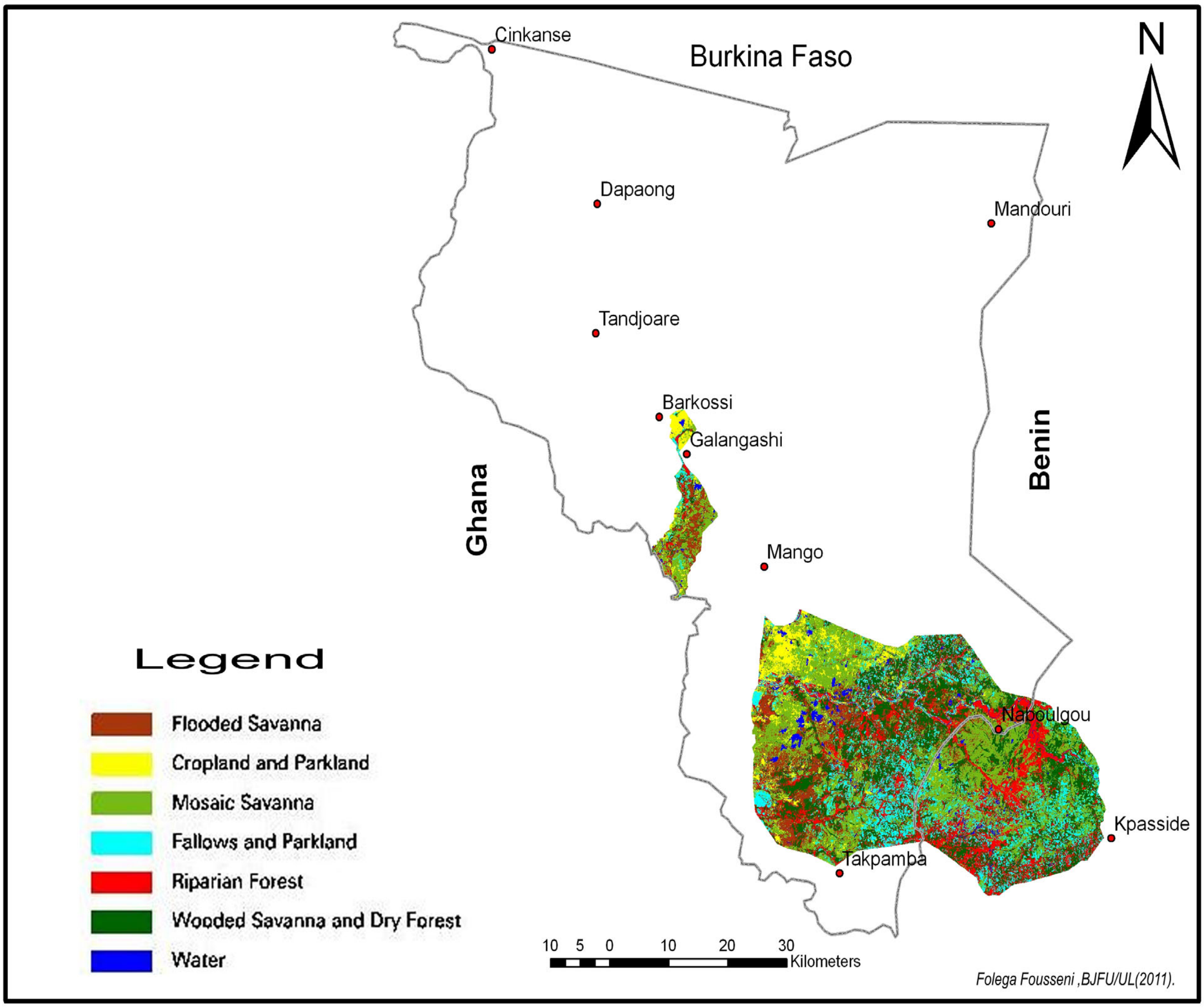

Fig. 3: Land cover map from 2007 ETM+ image in Barkoissi, Galangashi and Oti-Keran PA

Zones with minor or no change in vegetation (Fig. 2, Table 1) are represented by black, gray, and white colors on the map. Here the dynamics in vegetation are stable. However, negative NDVI values in black zones indicate water, barren soil, and villages. In gray and white areas, there is biomass, which is low in gray areas and very high in white areas. These few white areas correspond in particular to riparian forest and wooded savanna. Clearing of riparian forest and neighboring wooded savanna, such as dry forest, is clearly seen in the western part of the Oti-Keran protected area along the Koumongou River. Barren land and flooded areas (characterized by black) increase in this part of the reserve. From Table 1, the small extent of riparian forest and undisturbed vegetation is apparent.

Cyan (light blue), blue, green and magenta areas represent zones showing dynamic fluctuation (Fig. 2). These areas correspond roughly with the areas where the vegetation is in constant flux because of the interaction of clearing and regrowing process. Interpretation of areas in these colors allows the analysis of vegetation clearing, no-change, and regrowth classes in a time series (Hayes and Sader, 2002; Sader et al., 2003). Based on the semi-military management of the protected areas in Togo (Folega et al., 2011b) before 1990 and the loss of vegetation apparent before that date, it is likely that much more vegetation harvesting occurred after 1990.

Among the anthropogenic disturbances observed in the field, farming was the most common, followed by tree cutting and burning. The high pressure of these unceasing and increasing disturbances between 1990 and 2000, corroborate well with the high levels of vegetation loss during the same period.

The Barkoissi protected area illustrates this loss of vegetation well. Based on the results of ethno-botanical research (Pereki et al. 2010), the people on the borders of the protected area invaded the area over a period of 19 years for farming and harvesting. In this traditional system of land exploitation (Folega et al. 2011b; Wala et al. 2005), local residents deliberately preserved perennial, multipurpose, woody plants in association with their crops and breeding in a dispersed spatial arrangement. Today, this reserve appears more like an enormous range of parkland than a pro-

tected forest area.

However, estimation of loss and regrowth of vegetation is difficult in these fluctuating areas. Plant species regeneration in these protected areas has been higher than vegetation loss since the consensual rehabilitation of protected areas project was established (UICN/PACO, 2008). The Galangashi protected area provides better information on regrowth. Field studies here found that old fallow areas showed a progressive succession into shrubby and tree savanna.

Current land-cover types in the three protected area

Based on the digital image processing and visual interpretation of the imagery, seven classes of land cover were identified from differences in the spectral signature. These seven land cover typea covered 194903.6625 ha, which is greater than what has been mentioned in the literature (UICN/PACO, 2008).

A Kappa value of 0.67 represents a probable 67 percent better accuracy than if the classification resulted from a random unsupervised classification, according to the agreement criteria for the Kappa statistic defined by Antony and Joanne (2005). Thus, the classification can be considered as very good or substantially good. The overall accuracy is considered acceptable for this study.

However, there was some confusion among the seven classes from the error matrix. The confusion between cropland and parkland and mosaic savanna can be explained by the composite nature of some cropland and parkland previously in a fallow stage. Confusion between cropland and parkland and fallows and parkland was highly related to the agroforestry nature of these two classes; agroforestry practices are recurrent in this region. The class for wooded savanna and dry forest was close to that for riparian forest. But in the field, riparian forest growing along the meandering and temporary branches of the main rivers was easily confused with dry forests of *Anogeissus leiocarpus* (DC) Guill. and Perril and *Cissus populnea* Guill. and Perril.

Heterogeneity of croplands and parklands were also responsible for the confusion observed between this thematic class and riparian forest or flooded vegetation. This confusion can be linked to seasonality, since an area may be a pond in the rainy season (field observation in 2009), but only just wet during the dry season. Similarities in plant cover patterns, due to the logging of large trees by harvesters, was another source of confusion.

Previous research in this area, investigating biodiversity and plant community inventories (Folega et al. 2010; Dimobe 2009), has demonstrated the impact of anthropogenic disturbances on landscape features. The consequences of these disturbances are clearly visible in the Barkoissi protected area where cropland and parkland is the most important thematic class (Fig. 3). The removal and degradation of plant resources are also notably visible in the north, west, and south of the Oti-Keran protected area. However, these disturbances are also present in the Galangashi protected area, but this reserve is the best conserved and has suffered less from human disturbance.

Conclusions

A simple, fast and effective land-cover change detection technique was employed using RGB_NDVI classification on remote-sensing data. The substantial accuracy of the supervised classification output map could be useful for ecological monitoring of the area. Estimates of changes in land cover over time at the scale of the management unit could be useful for policy-makers with respect to conservation programs. However, this method could not fully explain land-cover dynamics in heterogeneous areas. Thus, further researches are needed in this area; among them can be quoted the forest and wooded vegetation inventory by remote sensing, vegetation monitoring, and carbon sequestration assessment. Within these drought areas of Togo, quantification of biomass and water stress is highly required in order to determine the potentiality of plant resource in the carbon mitigation through reducing emissions from deforestation and forest degradation (REDD+) guidelines as set the protocol Kyoto.

Acknowledgment
Authors greatly acknowledge the Chinese Ministry of Sciences and Technology -- the host of China-Africa Science and Technology Partnership Program (CASTEP) and the National Special Research Program for Forestry Welfare of China (201104009) whose have unconditionally fully support this research.

References

Afidegnon D, Caryon JL, Fromard F, Lakaze D, Guelly KA, Kokou K, Woegan AY, Batawila K. 2003. *Carte de la végétation du Togo: notice explicative*.UMR 5552/Université de Paul Sabatier, Faculté des Sciences /Université de Lomé.55.

Andrieu J, Mering C. 2008. Vegetation land cover change mapping of West African coastal zone from remotely sensed images: example of “Rivières-du-Sud” from Salum Delta (Senegal) to Rio Geba (Guinea-Bissau). *Revue Télédétection*, **8**(2): 93–118.

Anthony JV, Joanne MG. 2005. Understanding Interobserver Agreement: The Kappa Statistic. *Fam Med*, **37**(5): 360–363.

Baldyga TJ, Miller SN, Driese KL, Mainagichaba C. 2007. Land cover change assessment within Kenya’s Mau forest region using remotely sensed data. *Afr J Ecol,* **46**: 46–54.

Bayes T. 1763. An essay toward solving a problem in the doctrine of chances. *Philos T R Soc Lond,* **53**: 370–418.

Chavez PS, Mackinnon DJ. 1994. Automatic detection of vegetation changes in the Southwestern United States using remotely sensed images. *Photogramm Eng Rem S*, **60**: 571–583.

Chavez PS. 1996. Image-based atmospheric corrections—revisited and revised. *Photogramm Eng Rem S.,* **62**(9): 1025–1036.

Congalton RG. 1991. A review of assessing the accuracy of classifications of remotely sensed data. *Remote Sens Environ*, 37: 35–46.

Congalton RG, Green K. 1999. *Assessing the accuracy of remotely sensed data: principles and practices*. Boca Raton, Florida: CRC Press, pp.

45–48.

Dimobe K. 2009. Analyse de la dynamique spatiale des différentes formes de pressions anthropiques dans la réserve de l'Oti-Mandouri. Mem. DEA Biol .Veg. Appli. Univ. Lomé, Togo.

Ern H. 1979. *Die Vegetation Togo*. Gliederrung, Gefährdung, Erhaltung. Willdenowia, 9, pp.295–312.

Folega F, Zhao XH, Zhang CY, Wala K, Akpagana K. 2010. Ecological and numerical analyses of plant communities of the most conserved protected area in North-Togo. *Int J Biodvers Conserv,* **2**(11): 359–369.

Folega F, Zhang CY, Wala K, Zhao XH, Akpagana K. 2011a. Wooded vegetation of protected areas in Northern Togo. Case of Barkoissi, Galangashi and Oti-Keran: Ecological and Structure Analysis of Plant Communities. *Forestry Studies in China*, **13**(1): 23–35.

Folega F, Zhang CY, Samake, G, Wala K, Batawila K, Zhao XH, Akpagana K. 2011b**.** Evaluation of agroforestry species in potential fallows of areas gazetted as protected areas in north-Togo. *Afr J Agric Res,* **6**(12): 2828–2834.

Foody GM. 2002. Status of land cover classification accuracy assessment. *Remote Sens Environ,* **80**: 185–201.

Hayes DJ, Sader SA. 2002. Analyzing a forest conversion history database to explore the spatial and temporal characteristics of forest change. *Landscape Ecol,* **17**: 299–314.

Igue AM, Houndagba CJ, Gaiser T, Stahr K. 2006. Land use/cover map and its accuracy in the Oueme Basin of Benin (West Africa). Paper submitted to Conference on International Agricultural Research for Development. Tropentag, University of Bonn, October 11-13, 2006.4.

Jensen JR. 2005. *Introductory Digital Image Processing: A Remote Sensing Perspective*. 3rd Edition, Upper Saddle River: Prentice-Hall.

Kokou K, Sokpon N. 2006. Sacred forest in Dahomey gap. *Bois For Trop,* **288**(2): 15–23.

Kwarteng AY, Al-Ajmi D. 1996. Using Landsat Thematic Mapper data to detect and map vegetation changes in Kuwait. *International Archives of Photogrammetry and Remote Sensing,* **31**(B7): 398–405

Lillesand T, Kiefer R, Chipman J. 2008. *Remote Sensing and Image Interpretation*. 6th edition. NY: John Wiley & Sons.

Moussa A. 2008. Climate classification based on vegetation, rainfall and temperature (Togo). MEM Master of Geography, Université de Lomé, p.30.

Oba G, Post E, Stenseth NC. 2001. Sub-saharan desertification and productivity are linked to hemispheric climate variability. *Glob Change Biol,* **7**: 241–246.

Ola A. 2008. Extending post-classification change detection using semantic similarity metric to overcome class heterogeneity: A study of 1992 and 2001 US National Land Cover Databases changes. *Remote Sens Environ*, **112**: 1226–1241

Pereki H, Folega F, Batawila K, Wala K, Akpagana K. 2010. Reserve Barkoissi conversion in agroforestery parklands. *Int For Rev,* **12**(5): 193.

Rouse JW, Haas RH, Schell JA, Deering DW. 1974. Monitoring vegetation systems in the Great Plains with ERTS. *In*: *Third ERTS Symposium*. NASA SP-351 I, pp.309–317.

Sader SA, Winne JC. 1992. RGB-NDVI colour composites for visualizing forest change dynamics. *Int J Remote Sens*, **13**(16): 3055–3067.

Sader SA, Bertrand M, Wilson EH. 2003. Satellite change detection of forest harvest patterns on an industrial forest landscape. *Forest Sci,* **49**(3): 341–353

Sellers PJ. 1985. Canopy reflectance, photosynthesis, and transpiration. *Int J Remote Sens*, **6**: 1335–1372.

Sournia G, Alassoum O, Belemsobgo U, Djeri-Alassani B, Lartiges A, Sinsin B, Thomassey J. 1998. *French speaking countries protected areas*. Ed. ACCT/ Jean **–**Pierre de Monza.

Sun ZY, Ma R, Wang YX. 2009. Using Landsat data to determine land use changes in Datong basin, China. *Environ Geo*, **57**: 1825–1837.

Tchamie T. 1994. Lessons from the hostility of local people in respect of protected areas in Togo. *Unasylva*, **45**:176.

Tou J, Gonzalez R. 1974. *Pattern recognition principles.* London: Addison-Wesley.

Tucker CJ. 1979. Red and photographic infrared linear combinations for monitoring vegetation. *Remote Sens Environ*, **8**: 127–150

UICN/PACO. 2008. *Evaluation of effectiveness management of protected areas: protected areas in Togo*. ISBN: 978-2-8317-1130-0.44.

Wala K, Sinsin B, Guely AK, Kokou K, Akpagana K. 2005. Typology and structure of parkland in the prefecture of Doufelgou (Togo). *Sécheresse,* **16**(3): 209–216.

Westhoff V, van der Maarel E. 1978. The Braun-Blanquet Approach, 2nd ed. *In*: R.H. Whittaker (ed.). *Classification of Plant Communities*. The Hague: Junk, pp. 287–297.

Wilson EF, Sader SA. 2002. Detection of forest type using multiple dates of Landsat TM imagery. *Remote Sens Environ*, **80**: 385–396.

Yema E, Georges L. 1981. Togolese Association of Geographers Atlas of Togo (Les Atlas Jeune Afrique), Publishing J.A., 64: 58-59.